

Zeros of the $W_L Z_L \rightarrow W_L Z_L$ amplitude: where vector resonances stand

Alberto Filipuzzi, Jorge Portolés and Pedro Ruiz-Femenía

Departament de Física Teòrica, IFIC, CSIC — Universitat de València, Apt. Correus 22085, E-46071 València, Spain

(Dated: May 2, 2022)

A Higgsless electroweak theory may be populated by spin-1 resonances around $E \sim 1$ TeV as a consequence of a new strong interacting sector, frequently proposed as a tool to smear the high-energy behaviour of scattering amplitudes, for instance, elastic gauge boson scattering. Information on those resonances, if they exist, must be contained in the low-energy couplings of the electroweak chiral effective theory. Using the facts that: i) the scattering of longitudinal gauge bosons, W_L, Z_L , can be well described in the high-energy region ($E \gg M_W$) by the scattering of the corresponding Goldstone bosons (equivalence theorem) and ii) the zeros of the scattering amplitude carry the information on the heavier spectrum that has been integrated out; we employ the $\mathcal{O}(p^4)$ electroweak chiral Lagrangian to identify the parameter space region of the low-energy couplings where vector resonances may arise. An estimate of their masses is also provided by our method.

I. INTRODUCTION

LHC will conclude soon the search for the Standard Model (SM) Higgs boson below the TeV energy region. As up to now, with only a tiny open window of ~ 20 GeV, there are good chances that there will be no Higgs. If this is the case the search for the dynamics of the spontaneous symmetry breaking of the electroweak gauge symmetry will become a crucial goal of the high-energy physics research.

A Higgsless world would be most probably characterized by the presence of a new physics scale associated to a strong interacting sector lying around $E \sim 1$ TeV and related with the spontaneous breaking of the electroweak symmetry [1, 2]. A reasonable assumption, based on our knowledge of low-energy hadron physics, is that such a non-perturbative dynamics would lead to resonances that can be at the reach of future runs at the LHC or at an envisaged Linear Collider. It has also been argued that without a light Higgs the violation of perturbative partial-wave unitarity in the elastic scattering of the longitudinal components of those W or Z gauge bosons could be prevented by those spin-1 resonances [3] though this is by no means compulsory [2]. In this article we plan to investigate the possible existence of those vector resonances contributing to the $W_L Z_L \rightarrow W_L Z_L$ scattering process.

The symmetry breaking sector of the Standard Model without a Higgs becomes a non-linear sigma model with $SU(2)_L \otimes SU(2)_R / SU(2)_V$ symmetry where the $SU(2)_L \otimes U(1)_Y$ gauge symmetry is properly embedded. Interestingly enough the Lagrangian that describes it is the one of two-flavour Chiral Perturbation Theory (ChPT) [4, 5] with pions substituted by the Goldstone bosons that provide masses to the gauge bosons. ChPT is an effective field theory of Quantum Chromodynamics (QCD) at very low-energy, driven by the chiral symmetry of massless QCD, perturbative in momenta and valid for $p^2 \ll (4\pi F_\pi)^2$ (being F_π the decay constant of the pion), and renormalizable order by order in its perturbative expansion.

As in any effective field theory the low-energy coupling constants (LECs) of ChPT carry the information of the heavier spectra that has been left out in the procedure of constructing the low-energy theory. Indeed it has been shown that, at $\mathcal{O}(p^4)$, the LECs are saturated by the lightest hadron resonances [6]. In particular the two relevant LECs that appear

in the amplitude of the elastic pion-pion scattering are given by the contribution of the $\rho(770)$. Hence one can wonder if it would be possible to obtain the mass of the $\rho(770)$ from the values of those LECs. Of course it is not possible to establish the existence and properties of resonances using a perturbative framework. However one can provide procedures to resummate the perturbative contributions to the amplitude. We will translate one of these methods from the well studied QCD framework to the electroweak sector.

The procedure that we devise in order to explore the occurrence of spin-1 resonances in the $E \sim 1$ TeV region is based on the information about the spin-J resonances ($J \geq 1$) provided by the zeros of the scattering amplitude. This method goes back to the study of the zeros in $\pi\pi \rightarrow \pi\pi$ [7]. In Ref. [8] it was shown in the framework of ChPT that the zeros of the $I = 1$ $\pi\pi \rightarrow \pi\pi$ amplitude (I is short for the isospin quantum number) predict the mass of the $\rho(770)$ resonance when the chiral LECs are saturated by the resonance contributions. This shows that, though the ChPT amplitude is only valid for $p^2 \ll M_\rho^2$, the extrapolation provided by its zeros is to be trusted up to $E \sim M_\rho$.

The method can be applied to the electroweak sector employing the two following ingredients. First, the fact that the elastic scattering amplitude of the longitudinal components of the gauge bosons is given, at $E \gg M_W$, by the amplitude of the elastic scattering of the Goldstone bosons associated to the spontaneous electroweak symmetry breaking. This is known as the *equivalence theorem* and was devised originally to study those processes with a very heavy Higgs [2, 9]. The equivalence theorem thus allow us to trade the dynamics of the longitudinally polarized gauge bosons by the one of the corresponding Goldstone modes. And the second ingredient, already commented above, is the fact that the interactions among Goldstone bosons in the Higgsless electroweak theory is described, at least at leading order, by the two-flavour ChPT Lagrangian where now the multiplet of pions is substituted by the Goldstone fields that provide masses to the gauge bosons. The obvious difference is the relevant scale that rules the perturbative expansion of the amplitude [10–12]. Indeed the perturbative scale is now driven by $v \sim (\sqrt{2} G_F)^{-1/2} \simeq 246$ GeV with G_F the Fermi constant. Accordingly the effective theory is valid for $p^2 \ll (4\pi v)^2 \sim (3 \text{ TeV})^2$. Taking into account the equivalence theorem, the perturbative ex-

pansion and the Higgsless electroweak chiral effective theory (EChET) just mentioned, our working region is determined by $M_W \ll E \ll 4\pi v$.

We therefore exploit in this work the analogies between ChPT and Higgsless EChET and study the elastic scattering of the longitudinal components of the electroweak gauge bosons as described by the latter. Then, assuming that the LECs of the effective theory are saturated by the lightest vector resonances (if these exist) we determine the zeros of the amplitude and we explore the parameter space of the two only LECs that appear in the scattering amplitude, obtaining important information on the possible resonances.

The contents of this article are the following. In Section II we revisit the role of the zeros of an amplitude and its relation with the resonances of the theory. We will focus on the well known case of $\pi\pi \rightarrow \pi\pi$ scattering and the $\rho(770)$. In Section III we briefly review the Higgsless electroweak effective theory applied to the $W_L Z_L \rightarrow W_L Z_L$ scattering on which we will particularize our study. Section IV will be devoted to the analysis of the zeros of that amplitude and their interpretation as vector resonances. We will also discuss our results and the possibility left for LHC to disentangle the presence of these vector resonances. Our conclusions will be given in Section V. An Appendix reminds the reader the general conditions of convergence of the partial-wave expansion of the elastic $\pi\pi$ scattering amplitude.

II. THE ROLE OF THE ZEROS OF THE SCATTERING AMPLITUDE

We will now develop our method using QCD as the reference framework, taking advantage of the precise experimental data available and the good knowledge of the LEC values of $\mathcal{O}(p^4)$ ChPT used to describe the low-energy processes like $\pi\pi$ scattering. No conceptual changes will be needed to apply the method to the electroweak case.

The low-energy dynamics of elastic $\pi\pi$ scattering is determined by the existence of the lightest meson resonances contributing to that amplitude, $\sigma(600)$ and $\rho(770)$. Though the $\sigma(600)$ is mainly related with the chiral logs (it appears at next-to-leading order in the large number of colours (N_C) expansion), the information of the $\rho(770)$, leading in $1/N_C$, is encoded in the low-energy couplings at $\mathcal{O}(p^4)$ in the chiral expansion [6]. Within a quantum field theory approach, one can determine the resonance contributions to the chiral LECs starting from a Lagrangian with explicit resonance fields and then integrating them out. Typically those LECs are given in terms of the resonance couplings to the pions and inverse powers of the resonance masses.

One can wonder if the opposite procedure is viable. That is, if it would be possible to determine the mass of the resonances from the phenomenological determination of the LECs. As the ChPT amplitudes provide a perturbative expansion in momenta it is clear that the poles of resonances are not a feature of chiral symmetry. However a link between chiral dynamics and resonance contributions can be provided employing some ad-hoc resummation techniques like Padé approximants, the

inverse amplitude method or the N/D construction [13–15]. We will propose an alternative procedure based on the zeros of the scattering amplitude [7, 8, 16–18] as given by ChPT at $\mathcal{O}(p^4)$ (we will also comment on the next $\mathcal{O}(p^6)$ contribution).

Consider the amplitude $F(s, t)$ for $\pi^-(p_1)\pi^0(p_2) \rightarrow \pi^-\pi^0$ in the s-channel:

$$s = (p_1 + p_2)^2, \quad t = \frac{1}{2}(s - 4M_\pi^2)(\cos\theta - 1). \quad (1)$$

This amplitude has no $I = 0$ component, and from the phenomenology we know that the isovector P-wave is large whereas the $I = 2$ (exotic) S-wave is small. We can anticipate that these features are essential for our method. The P-wave is dominated by the $\rho(770)$ resonance and therefore around this energy region we can write the partial-wave expansion of the amplitude as:

$$F(s, t) = 16\pi f_0^2(s) + \frac{48\pi}{\sigma} \frac{M_\rho \Gamma_\rho(s)}{M_\rho^2 - s - iM_\rho \Gamma_\rho(s)} \cos\theta + \dots, \quad (2)$$

where $\sigma = \sqrt{1 - 4M_\pi^2/s}$ and $f_\ell^I(s)$ is the partial-wave with isospin I and angular momentum ℓ , defined through the partial-wave expansion of the s-channel amplitude with defined isospin:

$$F^I(s, t) = 32\pi \sum_{\ell=0}^{\infty} (2\ell + 1) f_\ell^I(s) P_\ell(\cos\theta), \quad (3)$$

with $P_\ell(z)$ the Legendre polynomial of degree ℓ . Unitarity imposes severe constraints on the structure of the partial-waves $f_\ell^I(s)$. A description consistent with unitarity is given by

$$f_\ell^I(s) = \frac{1}{\sigma} e^{i\delta_\ell^I} \sin\delta_\ell^I, \quad (4)$$

with δ_ℓ^I the phase shift of isospin I and angular momentum ℓ , that is real for elastic scattering.

The remaining terms not quoted in Eq. (2) amount to numerically suppressed higher partial waves. Taking into account the small size of the S-wave component, the angular distribution associated to $F(s, t)$ would have a marked dip at $\cos\theta = 0$, where also $F(s, t) \simeq 0$. This reflects the spin-1 nature of the $\rho(770)$. Due to the properties of the Legendre polynomials these dips in the angular distribution (or zeros of the amplitude) will appear for $\ell > 0$ and their number in the physical region, $\cos\theta \in [-1, 1]$, will be given by the angular momentum of the partial-wave. These zeros can be considered as dynamical features which give the spin to the resonance.

This observation gives us a possible path to analyze the spectrum of $J \geq 1$ resonances integrated out and hidden in the couplings of the effective field theory. Let us specify several features of the zeros of the amplitude and give precise definitions that will help to fix our procedure.

Being analytical functions of more than one variable the zeros of the amplitude are not isolated but continuous, defining a one-dimensional manifold for real s and complex t . Using Eq. (1) the $F(s, t)$ amplitude in the s-channel may be expressed as $F(s, z)$ with $z \equiv \cos\theta$. Then the solution of $F(s, z_0) = 0$ for physical values of the s variable is defined by

$z = z_0(s)$. Though the zeros of the function happen at complex values of the z variable, we define the *zero contour* as the real part of the zeros ($\text{Re } z_0(s)$). It is also phenomenologically observed [19, 20] that this contour continues smoothly from one region to another in the Mandelstam plane¹. Using Eqs. (2,4) we get:

$$z_0(s) = -\frac{e^{i\delta_0^2} \sin \delta_0^2}{3 M_\rho \Gamma_\rho(s)} (M_\rho^2 - s - i M_\rho \Gamma_\rho(s)) . \quad (5)$$

In the narrow resonance approximation (dropping $\Gamma_\rho(s)$ in the numerator of Eq. (5)) we see that $z_0(M_\rho^2) = 0$. For a finite $\rho(770)$ width we have:

$$\text{Re } z_0(s) = -\frac{\sin 2\delta_0^2}{6 M_\rho \Gamma_\rho(s)} (M_\rho^2 - s) - \frac{1}{3} \sin^2 \delta_0^2 , \quad (6)$$

that satisfies $|\text{Re } z(M_\rho^2)| \leq \frac{1}{3}$. In fact, and due to

the exotic character of the S-wave $I = 2$ background ($\text{Im } f_0^2(s) \ll \text{Re } f_0^2(s)$) and to the absence of the S-wave $I = 0$ channel, we know that $|\text{Re } z(M_\rho^2)| \ll \frac{1}{3}$.

Hence, for a generic amplitude where the P-wave contribution dominates and is saturated by a vector resonance, the resonance mass M_R should be found as the solution of:

$$\text{Re } z_0(M_R^2) \simeq 0 , \quad (7)$$

where $z_0(s)$ is the zero contour obtained from that amplitude. We will take this condition as our source of information on the resonances given by $F(s, t)$. It is clear, from Eq. (2), that how deep is the dip of the angular distribution will also depend on the size of the imaginary part of the zeros. We will comment on this point further in Section IV.

Let us repeat (and update) now the procedure in Ref. [8], showing how the method developed works in a real case. The $\mathcal{O}(p^4)$ amplitude of $\pi^- \pi^0 \rightarrow \pi^- \pi^0$, with the variables defined in Eq. (1), is given by [5]:

$$\begin{aligned} A(t, s, u) = & \frac{t - M^2}{F^2} + \frac{1}{6 F^4} \left[3(t^2 - M^2) \bar{J}(t) + [s(s - u) - 2 M^2 s + 4 M^2 u - 2 M^4] \bar{J}(s) \right. \\ & \left. + [u(u - s) - 2 M^2 u + 4 M^2 s - 2 M^4] \bar{J}(u) \right] \\ & + \frac{1}{96 \pi^2 F^4} \left[2 \left(\bar{\ell}_1 - \frac{4}{3} \right) (t - 2 M^2)^2 + \left(\bar{\ell}_2 - \frac{5}{6} \right) (t^2 + (s - u)^2) - 12 M^2 t + 15 M^4 \right] , \end{aligned} \quad (8)$$

where F is the decay constant of the pion in the chiral limit, $F \simeq F_\pi \simeq 92.4 \text{ MeV}$ and $M \simeq M_\pi \simeq 138 \text{ MeV}$. The one-loop $\bar{J}(x)$ function was defined in Ref. [5]. $\bar{\ell}_1$ and $\bar{\ell}_2$ are a priori unknown low-energy couplings related with those of the $\mathcal{O}(p^4)$ ChPT Lagrangian with two flavours, $\ell_i^r(\mu)$ ($i = 1, 2$), through:

$$\begin{aligned} \ell_1^r(\mu) &= \frac{1}{96 \pi^2} \left(\bar{\ell}_1 + \ln \frac{M_\pi^2}{\mu^2} \right) , \\ \ell_2^r(\mu) &= \frac{1}{48 \pi^2} \left(\bar{\ell}_2 + \ln \frac{M_\pi^2}{\mu^2} \right) . \end{aligned} \quad (9)$$

Here μ is the renormalization scale. With these definitions the $\bar{\ell}_i$ couplings are, but for a factor, equal to $\ell_i^r(M_\pi^2)$ and thus scale independent. It is well known [6] that the $\mathcal{O}(p^4)$ chiral LECs are saturated by the contribution of the lightest resonances that have been integrated out. In fact, $\ell_1^r(\mu)$ and

$\mu(\text{GeV})$	0.6	0.77	0.9
$\bar{\ell}_1$	-0.33	0.25	0.58
$\bar{\ell}_2$	4.46	5.03	5.37
$10^5 r_5^V$	5.55	4.96	4.78
$10^5 r_6^V$	0.67	0.86	0.94

TABLE I. Renormalization scale dependence of the LECs determinations relevant for the evaluation of the zero contours at $\mathcal{O}(p^4)$ and $\mathcal{O}(p^6)$ in ChPT.

$\ell_2^r(\mu)$ are saturated by the lightest multiplet of vector resonances. Upon resonance integration at tree level one gets the three-flavour LECs $L_i^r(\mu)$. Using the $\mathcal{O}(p^4)$ matching with the two-flavour $\ell_i^r(\mu)$ [22], the resonance contributions to the latter read $\ell_1^r(\mu) = -G_V^2/M_V^2 - \nu_K/24$ and $\ell_2^r(\mu) = G_V^2/M_V^2 - \nu_K/12$. Here $M_V \simeq M_\rho$ is the mass of the lightest nonet of vector resonances, and G_V is a coupling of the Resonance Chiral Theory phenomenological Lagrangian [6]. Its value is estimated as $G_V \in [40, 50] \text{ MeV}$ [23, 24] and we take $G_V \simeq 45 \text{ MeV}$ for the numerical evaluation. In addition $\nu_K = (\ln(M_K^2/\mu^2) + 1)/(32\pi^2)$. The constants $\bar{\ell}_i$ become μ -dependent if we substitute the $\ell_i^r(\mu)$ in Eq. (9) by the tree-level estimates above. It is generally assumed that vector resonance saturation of the low-energy constants implies that the

¹ There is one known situation where this is not the case and the contours wiggle. This happens when they pass a threshold that opens strongly in the S-wave. One such example is the $K\bar{K}$ threshold in $I = 0 \pi\pi$ scattering [21]. As we consider here the $\pi^- \pi^0$ channel, which has no isoscalar component, we expect the zero contour to be quite smooth well beyond the $\rho(770)$ mass.

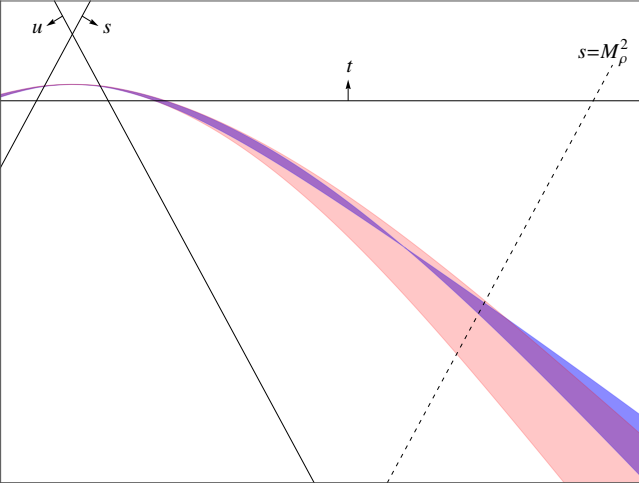


FIG. 1. Zero contours of $\pi^-\pi^0 \rightarrow \pi^-\pi^0$ at $\mathcal{O}(p^4)$ (light colour) and $\mathcal{O}(p^6)$ (dark colour) in the Mandelstam plane. The bands correspond to the range of LECs for $\mu = 0.6$ GeV and $\mu = 0.9$ GeV as given in Table I. The zero contours connect with the Weinberg's projection of the Adler zero inside the Mandelstam triangle [25].

resonance contributions determine the LECs quite well for a scale μ of the order of the mass of the resonance. Within the interval $\mu \in [0.6, 0.9]$ GeV, the couplings $\bar{\ell}_1$ and $\bar{\ell}_2$ take the values shown in Table I; for the central value, $\mu = M_\rho$, one gets $\bar{\ell}_1 = 0.25$, $\bar{\ell}_2 = 5.03$. With these estimates, we can readily evaluate the zero contour from the $\mathcal{O}(p^4)$ ChPT, and obtain the $\rho(770)$ mass through Eq. (7). In the Mandelstam plane the outcome for the zero contours takes the form of the lighter band in Figure 1, whose limits are given by the extreme values of $\bar{\ell}_1$ and $\bar{\ell}_2$ in Table I. These zero contours intersect the $\text{Re } z$ -axis for $M_R \in [0.69, 0.91]$ GeV. The estimate is particularly good for the central value $\mu = M_\rho$, which yields $M_R = 0.75$ GeV. Let us note that the μ -dependence of the zero contour prediction for the $\rho(770)$ mass does not reflect any uncertainty intrinsic to the method, but is just a consequence of the incomplete knowledge of the resonance estimates of the LECs.

We would like next to show how the zero contour in Figure 1 changes when the next chiral order is considered. The $\pi^-\pi^0 \rightarrow \pi^-\pi^0$ amplitude up to $\mathcal{O}(p^6)$ has been computed in Ref. [26]. At this order the result depends on 6 low-energy couplings $r_i^r(\mu)$, $i = 1, \dots, 6$. Assuming that the values of the latter are saturated by vector resonance contributions, one can get estimates for $r_i^r(\mu) \simeq r_i^V$ [26] in the same way as for the $\ell_i^r(\mu)$. We take the values of r_i^V , $i = 1, 2, 3, 4$, as given in [26]. However we have an updated evaluation for $i = 5, 6$, obtained as follows: we use the definition of r_5^V and r_6^V in terms of the $\mathcal{O}(p^6)$ two-flavour LECs $c_i^r(\mu)$ [27], then the relation of the two-flavour LECs with the three-flavour ones $C_i^r(\mu)$ [28], and finally we determine the latter by integrating the resonance fields at tree-level [29]. Incidentally only vector resonances contribute to r_5^V and r_6^V . The numerical values of r_5^V and r_6^V that we get, shown in Table I, are typically a factor of 2 to 4 smaller than the ones quoted in Ref. [26]. This proce-

dure cannot be applied, at the moment, for r_i^V , $i = 1, 2, 3, 4$, because the conversion between the corresponding LECs with two and three flavours has not been made available yet. The obtained $\mathcal{O}(p^6)$ zero contours are displayed by the darker band of Figure 1, that is defined by the μ -dependent values of the LECs given in Table I. The $\rho(770)$ mass estimates from these $\mathcal{O}(p^6)$ zero contours read $M_R \in [0.83, 1.01]$ GeV. We notice that the resonance estimate of r_4^V involves a cancellation of two different contributions of similar size. If we, for instance, change the sign of r_4^V the $\rho(770)$ mass estimates at $\mathcal{O}(p^6)$ are shifted to $M_R \in [0.79, 0.90]$ GeV. The strong dependence of these determination on the values of the $r_i^r(\mu)$ (specially on $r_4^r(\mu)$ and $r_6^r(\mu)$) calls for an updated evaluation of the latter before assessing the validity of the zero contour approach at $\mathcal{O}(p^6)$ for the case of the $\rho(770)$.

The zero contours provide also an alternative unitarization procedure for the ChPT amplitude. Indeed assuming that the amplitude satisfies the partial-wave expansion (3) and neglecting $\ell \geq 2$ partial waves one obtains:

$$\tan \delta_1^1(s) = \frac{-\frac{1}{2} \sin 2\delta_0^2(s)}{3 \text{Re } z_0(s) + \sin^2 \delta_0^2(s)}. \quad (10)$$

Note that, if the S-wave $I = 2$ phase-shift is small, the P-wave phase shift δ_1^1 will pass through $\pi/2$ when $\text{Re } z_0(s) \rightarrow 0$, thus indicating the presence of a resonance. The zero contour provided by the $\mathcal{O}(p^4)$ ChPT amplitude could then be employed to obtain the contribution of the lightest vector resonance (the $\rho(770)$ in the QCD case) to the $\delta_1^1(s)$ phase shift. This is by no means evident. The chiral expansion provides an accurate description at very low energies only, namely for $E \ll M_\rho$. Hence the fact that the zero contour is able to unitarize the theory at $E \sim M_\rho$ has to rely on the properties of those zero contours.

In Figure 2 we compare the experimental data on the $\delta_1^1(s)$ phase-shift from elastic $\pi\pi$ scattering with different theoretical predictions. As expected the prediction given by the ChPT amplitude does not provide the right description for $E \sim M_\rho$, as can be seen looking at the dot dashed line that represents the ChPT result for the P-wave phase-shift, namely $\delta_1^1(s) = \sigma \text{Re } f_1^1(s)$ [33]. On the other hand the $\delta_1^1(s)$ phase-shift as given by (10) is in much better agreement with experimental data. We plotted the theoretical results for two different $I = 2$ S-wave phase-shift representations, the one coming from the $\mathcal{O}(p^4)$ ChPT result (dashed line) and the one given by the Schenk parameterization [34] (continuous line). As it can be seen the latter provides a much better agreement to the data in the low-energy region, however the pass through $\pi/2$ depends little on the parameterization used for $\delta_0^2(s)$.

In summary, we have seen that the zeros of the amplitude of elastic $\pi\pi$ scattering carry important dynamical information on the structure of the interaction, in particular the role of spin-1 resonances. This information, encoded in the low-energy couplings of $\mathcal{O}(p^4)$ ChPT, emerges through the zero contour definition and the condition in Eq. (7). Alternatively the unitarization in Eq. (10) is able to show the mark of the $\rho(770)$ in the $\delta_1^1(s)$ phase-shift, as we demonstrated in Figure 2. This is not a trivial exercise because the results of ChPT are only valid for $E \ll M_\rho$, however the smoothness

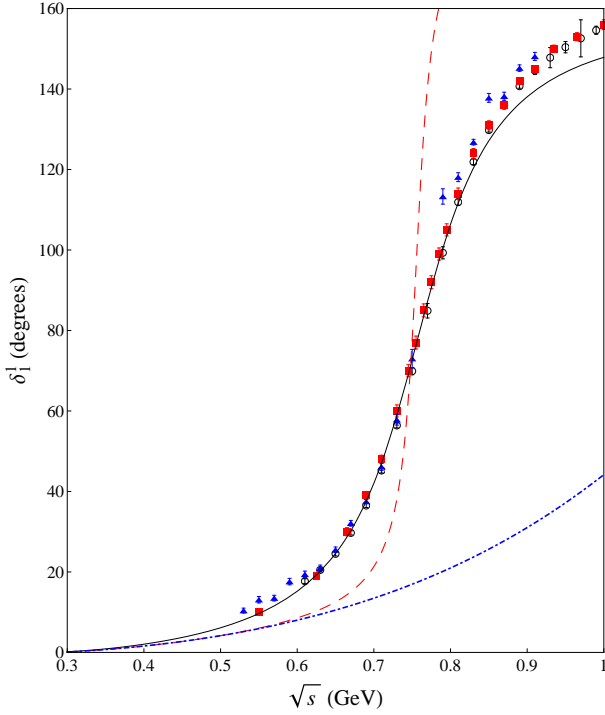


FIG. 2. $\delta_1^1(s)$ phase-shift in elastic $\pi\pi$ scattering. Comparison of experimental data [30–32] with the prediction given by Eq. (10) for the S-wave given by the Schenk parameterization (continuous line) and by $\mathcal{O}(p^4)$ ChPT (dashed line). The $\mathcal{O}(p^4)$ ChPT result for the P-wave phase-shift, namely $\delta_1^1(s) = \sigma \text{Re} f_1^1(s)$, is also shown (dot-dashed line).

of the zero contour and its stability under unitarization procedures [18, 35], collaborate to disentangle the information of the LECs, at least in the channel we are considering.

III. THE ELECTROWEAK CHIRAL LAGRANGIAN

In the absence of a Higgs, a strong interacting sector responsible for providing masses to the electroweak gauge bosons is described by Goldstone bosons π^a , $a = 1, 2, 3$, associated to the $SU(2)_L \otimes U(1)_Y \rightarrow U(1)_{\text{em}}$ spontaneous symmetry breaking, which become the longitudinal components of the electroweak gauge bosons. The corresponding EChET Lagrangian is then described by the non-linear sigma model based on the coset $SU(2)_L \otimes SU(2)_R / SU(2)_{L+R}$ where $SU(2)_L \otimes U(1)_Y$ is gauged. The $SU(2)_{L+R} \equiv SU(2)_C$ is the custodial symmetry that is usually enforced in order to keep the relation $M_W = M_Z \cos \theta_W$ and the smallness of the T oblique parameter.

A convenient parameterization of the Goldstone fields is given by:

$$U(x) = \exp \left(\frac{i}{v} \pi^a \tau^a \right), \quad (11)$$

with τ^a the Pauli matrices. This transforms as LUR^\dagger , with $L \in SU(2)_L$ and $R \in U(1)_Y$, under the gauge group. Up to

dimension four operators, the most general $SU(2)_L \otimes U(1)_Y$ gauge invariant and CP-invariant Lagrangian which implements the global symmetry breaking $SU(2)_L \otimes SU(2)_R$ into $SU(2)_{L+R}$ in the limit when g' vanishes², is given by the terms [10–12]:

$$\mathcal{L}_{\text{EChET}} = \frac{v^2}{4} \langle (D_\mu U)^\dagger D^\mu U \rangle + \sum_{i=0, \dots, 5} a_i \mathcal{O}_i, \quad (12)$$

with the operators:

$$\begin{aligned} \mathcal{O}_0 &= g'^2 \frac{v^2}{4} \langle T V_\mu \rangle^2, \\ \mathcal{O}_1 &= \frac{igg'}{2} B^{\mu\nu} \langle T W_{\mu\nu} \rangle, \\ \mathcal{O}_2 &= \frac{ig'}{2} B^{\mu\nu} \langle T [V^\mu, V^\nu] \rangle, \\ \mathcal{O}_3 &= i g \langle W_{\mu\nu} [V^\mu, V^\nu] \rangle, \\ \mathcal{O}_4 &= \langle V_\mu V_\nu \rangle^2, \\ \mathcal{O}_5 &= \langle V_\mu V^\mu \rangle^2, \end{aligned} \quad (13)$$

where $V_\mu = (D_\mu U) U^\dagger$, $T = U \tau^3 U^\dagger$. The covariant derivative takes the form:

$$D_\mu U = \partial_\mu U + \frac{i}{2} g \tau^k W_\mu^k U - \frac{i}{2} g' \tau^3 U B_\mu, \quad (14)$$

with $W_{\mu\nu} = \tau^k W_{\mu\nu}^k/2$, and being $W_{\mu\nu}^k$ and $B_{\mu\nu}$ the gauge field strength tensors. In Eqs. (12,13) $\langle \dots \rangle$ denotes the trace in the $SU(2)$ space. Other 8 possible operators, that violate custodial symmetry when $g' \rightarrow 0$ (see *e.g.* [15]), will not be considered here. $\mathcal{L}_{\text{EChET}}$ involves a perturbative derivative expansion as ChPT does, driven this time by the scale $\Lambda_{\text{EW}} = 4\pi v \simeq 3 \text{ TeV}$, *i.e.* an expansion in powers of $(p^2, M_V^2)/\Lambda_{\text{EW}}$.

The first term in the Lagrangian (12) has dimension two, and provides the SM mass terms for the gauge bosons. The rest of terms are dimension 4 operators, and only \mathcal{O}_{3-5} are relevant for the purposes of our work. \mathcal{O}_3 represents an anomalous triple gauge-boson coupling while \mathcal{O}_4 and \mathcal{O}_5 give anomalous quartic gauge-boson interactions. The corresponding low-energy couplings a_3 , a_4 and a_5 encode the information of the heavier spectrum that has been integrated out in order to get $\mathcal{L}_{\text{EChET}}$. They are the analogous to the chiral LECs $\ell_i^T(\mu)$ discussed in Section II.

A. Longitudinally polarized gauge boson scattering

In this work we are interested in the scattering of vector bosons with longitudinal polarization because is the one linked, through the Higgs mechanism, with the Goldstone bosons of the electroweak symmetry breaking sector. The exact relation is provided by the *equivalence theorem* [2, 9]:

$$A(V_L^a V_L^b \rightarrow V_L^c V_L^d) = A(\pi^a \pi^b \rightarrow \pi^c \pi^d) + \mathcal{O}\left(\frac{M_V}{E}\right), \quad (15)$$

² Recall that the $U(1)_Y$ interactions explicitly break the global $SU(2)_L \otimes SU(2)_R$ and the custodial $SU(2)_{L+R}$ symmetries.

which states that, at center of mass energies $E \gg M_V$, the amplitude for the elastic scattering of longitudinally polarized vector bosons (V_L^a) equals the amplitude where the gauge fields have been replaced by their corresponding Goldstone bosons (π^a). Now, we can use the electroweak effective Lagrangian (12) to calculate the amplitude of Goldstone boson scattering of Eq. (15). Since the effective Lagrangian formalism is a low-energy expansion, some care is needed to apply the equivalence theorem, which is valid in the high-energy limit. The restricted version of the theorem which applies to the gauge boson scattering amplitude calculated at $\mathcal{O}(p^4)$ reads [36]:

$$A(V_L^a V_L^b \rightarrow V_L^c V_L^d) = A^{(4)}(\pi^a \pi^b \rightarrow \pi^c \pi^d) + \mathcal{O}\left(\frac{M_V}{E}\right) + \mathcal{O}(g, g') + \mathcal{O}\left(\frac{E^5}{\Lambda_{\text{EW}}^5}\right), \quad (16)$$

where $A^{(4)}$ is the amplitude of Goldstone boson scattering at lowest order in the electroweak couplings (g and g') as obtained from the effective Lagrangian $\mathcal{L}_{\text{EChET}}$. Therefore only the operators \mathcal{O}_4 and \mathcal{O}_5 in Eq. (13) contribute to that amplitude, which is linear in the a_4 and a_5 couplings. Let us remark that at $\mathcal{O}(g^0, g'^0)$ the masses of the gauge bosons vanish and the equivalence theorem, as given by Eq. (16), indicates that the Goldstone boson scattering amplitude has to be calculated in the zero mass limit. Mass corrections appear in the neglected terms.

Notice that the restricted version given by Eq. (16) is valid in the energy range given by $M_V \ll E \ll \Lambda_{\text{EW}}$. Since the EChET framework is analogous to ChPT, and the latter works reasonably well up to $500 \text{ MeV} \simeq 2\pi F_\pi$, we can assume that the effective formalism for the electroweak theory is limited at about $2\pi v \simeq 1.5 \text{ TeV}$. Given the success of the zero-contour method for the case of the $\rho(770)$ resonance, whose mass is larger than the limit of validity of the theory, the range above may be extended up to $E \lesssim 2 \text{ TeV}$, at least for what concerns the determination of the resonance mass through the zero contours.

IV. ANALYSIS OF THE ZEROS OF THE $W_L Z_L \rightarrow W_L Z_L$ AMPLITUDE

The equivalence theorem pointed out in the last section can be used to relate, at leading order, the amplitude of $W_L Z_L \rightarrow W_L Z_L$ with the one of the corresponding Goldstone bosons, which is analogous to the $\pi^- \pi^0 \rightarrow \pi^- \pi^0$ amplitude described in Section II. Notice that the physical system provided by the Higgsless Lagrangian in Eq. (12) is, but for the change of scale ($F_\pi \rightarrow v$), the same than the one of the ChPT. Therefore one would expect a similar dynamics if the P-wave contribution is saturated by a vector resonance. Consequently we could apply the same procedure and study the occurrence of $I = 1$ vector resonances³ in the scattering $W_L Z_L \rightarrow W_L Z_L$ through the

analysis of the zero contours of the EChET amplitude. As explained in Section II, zero contours cross the resonance location close to where the Legendre polynomial vanishes, which for vector resonances amounts to the condition (7).

By virtue of the equivalence theorem, the amplitude for $W_L Z_L \rightarrow W_L Z_L$ is equal, up to $\mathcal{O}(p^4)$ terms, to $A^{(4)}(\pi^- \pi^0 \rightarrow \pi^- \pi^0) = A(t, s, u)$ in Eq. (8), with the trivial replacements:

$$F \rightarrow v, \quad (\bar{\ell}_1, \bar{\ell}_2) \rightarrow (\bar{a}_5, \bar{a}_4).$$

In addition, the limit $M \rightarrow 0$ has to be performed, according to the restricted form of the theorem. This amounts to writing $M = 0$ in the polynomial contributions in $A(t, s, u)$. Care has to be taken in the one-loop functions, where keeping the leading order in that limit leaves a mass dependence in the logarithms. The scale-independent \bar{a}_i couplings are related to their renormalized counterparts in the $\overline{\text{MS}}$ scheme as:

$$a_4^r(\mu) = \frac{1}{4} \frac{1}{48\pi^2} \left(\bar{a}_4 - 1 + \ln \frac{M_W^2}{\mu^2} \right), \\ a_5^r(\mu) = \frac{1}{4} \frac{1}{96\pi^2} \left(\bar{a}_5 - 1 + \ln \frac{M_W^2}{\mu^2} \right). \quad (17)$$

This definition for $a_4^r(\mu)$ and $a_5^r(\mu)$ differs from that of Eq. (9) that relates the $\ell_i^r(\mu)$ to the $\bar{\ell}_i$; it matches though the definition used in recent literature [37, 38] for these couplings, so it is adopted here to make contact with those results. The natural order of magnitude of the couplings is $\bar{a}_{4,5} \sim \mathcal{O}(1)$, so we can expect that $a_i^r \sim \mathcal{O}(10^{-3})$.

Recalling the procedure that we used in Section II, we will look for the zero contours of the amplitude, $A^{(4)}(s, z_0) = 0$, and identify the vector resonances with solutions of $\text{Re } z_0(M_R^2) = 0$. However we still need to impose another constraint on this result to ensure that the assumptions leading to condition (7) are fulfilled. As it was seen in Section II, our procedure depends crucially, after neglecting higher partial waves, on having a dominant resonance-saturated P-wave and a small, non-vanishing, S-wave contribution. We can translate this requirement to a numerical bound in the following way. Writing the equation $A^{(4)}(s, z_0) = 0$ in terms of its partial-wave series, one gets:

$$f_0^2(s) + 3 f_1^1(s) z_0(s) \simeq 0, \quad (18)$$

if higher-order partial waves are neglected. At the resonance location, $s = M_R^2$, the latter equation relates the size of the imaginary part of the zero with the ratio between the S- and the P-wave contributions:

$$|z_0(M_R^2)| = |\text{Im } z_0(M_R^2)| = \left| \frac{f_0^2(M_R^2)}{3 f_1^1(M_R^2)} \right| < \lambda. \quad (19)$$

The bound λ then defines the range of applicability of our method: zeros of the amplitude with imaginary part smaller than λ can be considered positive results in the search for vector resonances. The zeros which pass this condition bear a similarity to the near-by zeros introduced in the pioneering works on zero contours, characterized by small imaginary parts. A reference value for λ can be inferred from the $\rho(770)$

³ Isospin, in the context of the Lagrangian (12), indicates the quantum number associated to the unbroken $SU(2)_{L+R}$ custodial symmetry.

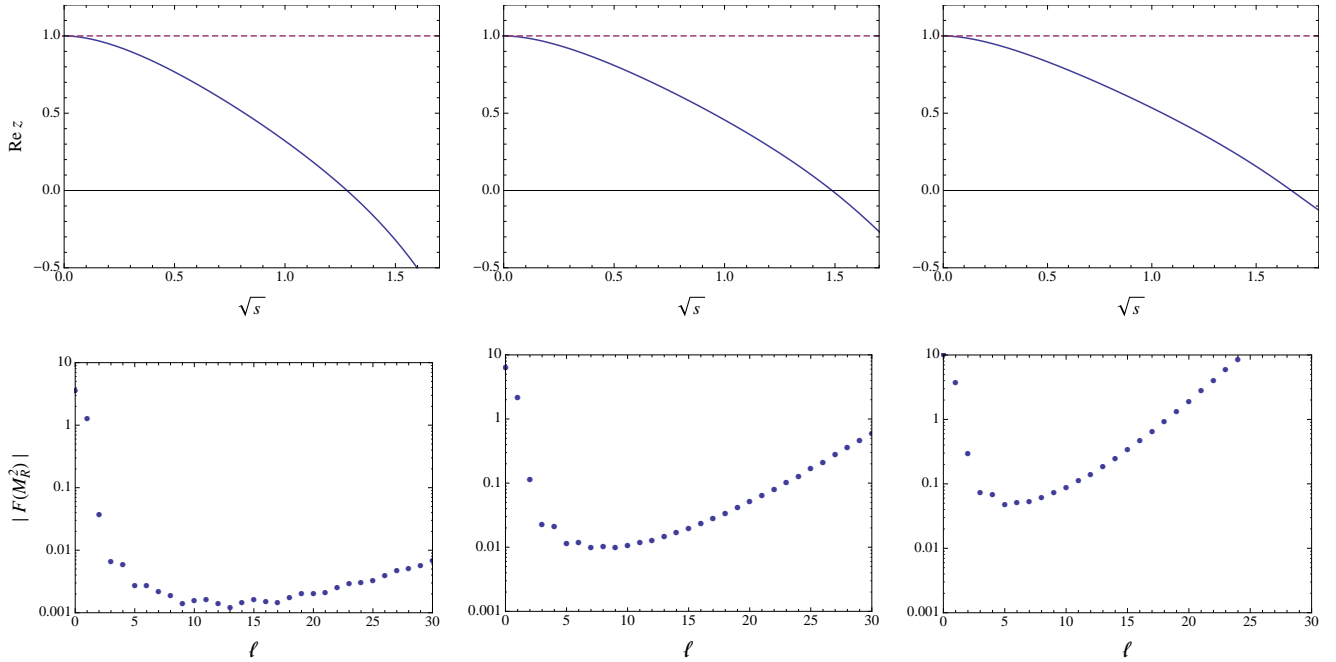


FIG. 3. Upper panels: Zero contours from the $\mathcal{O}(p^4)$ amplitude for, from left to right, $(\bar{a}_4, \bar{a}_5) = (10, 10)$, $(\bar{a}_4, \bar{a}_5) = (8.5, 10)$ and $(\bar{a}_4, \bar{a}_5) = (7.7, 10)$. The dashed line are the amplitude zeros obtained from the lowest order chiral amplitude. Lower panels: Corresponding $\mathcal{O}(p^4)$ amplitudes $|F(M_R^2)| \equiv |A^{(4)}(M_R^2, z_0(M_R^2))|$ (in logarithmic scale) for the upper panel cases, using the partial-wave expansion up to order ℓ .

case studied in Section II, where one gets $|\text{Im } z_0(M_R^2)| \simeq 0.36$ (for $\mu = 0.77$ GeV; see Table I). For values of λ larger than $1/2$ we cannot consider the S-wave to be significantly smaller than the P-wave, and we therefore choose $\lambda = 1/2$ as a limiting value for the identification of resonances in the zero contours. The dependence of our results on this cut is discussed later.

The λ -cut in Eq. (19) is also related with the convergence of the partial-wave expansion of the amplitude. For the zero mass case the partial-wave expansion is convergent only in the physical region, i.e. for $z \equiv \cos \theta \in [-1, 1]$ (see Appendix A). The partial-wave series continued to complex values of z is at best asymptotically convergent. Hence smaller imaginary parts of the zeros imply a better behaviour of the series. In the lower panels of Figure 3 we show the convergence of the partial-wave series at $s = M_R^2$ for three representative examples, corresponding (from left to right) to $(\bar{a}_4, \bar{a}_5) = (10, 10)$, $(8.5, 10)$, $(7.7, 10)$, with non-zero imaginary parts given by $|\text{Im } z_0(M_R^2)| \simeq 0.26, 0.39$ and 0.56 , respectively. As can be seen there is a direct correlation between the size of the imaginary part of $z_0(M_R^2)$ and the convergence of the expansion. Note also that the minimal value of the amplitude at the resonance location gets closer to zero for smaller $|\text{Im } z_0(M_R^2)|$. The corresponding zero contours, obtained from the amplitude (8) (now keeping only the leading order in the $M \rightarrow 0$ limit), are smooth lines in the $(\text{Re } z, s)$ plane, as shown in the upper panels of Figure 3. The dashed line are the amplitude zeros obtained from the lowest order chiral amplitude, which are simply given by $t = 0$ and thus

lie on a straight line in the Mandelstam plane. In terms of z the $\mathcal{O}(p^2)$ zeros are given by $z_0(s) = 1$ and have no imaginary part because the $\mathcal{O}(p^2)$ amplitude is real. The $\mathcal{O}(p^4)$ corrections induce an imaginary part in the zero trajectories, and are essential to bend down the zero contour towards $\text{Re } z = 0$. The crossing, from left to right in Figure 3, takes place at $M_R \simeq 1.28, 1.49$ and 1.67 TeV.

Figure 4 is the central result of our work. The shaded areas show where resonances, defined by the conditions (7) and (19) with $\lambda = 1/3$, are found in the (\bar{a}_4, \bar{a}_5) -plane. The contour lines drawn correspond to pairs of (\bar{a}_4, \bar{a}_5) which yield the same resonance mass. Though the validity of the approach cannot be trusted beyond $E \simeq 2$ TeV, we have displayed in the plot resonances found with masses up to 2.5 TeV. In order to show how dependent are the solutions from Eq. (7) to the cut (19) on the imaginary part of the zeros, we have also drawn in Figure 4 (outer dashed line) the boundary of the region yielding resonances when $\lambda = 1/2$. The hatched region in the left and lower parts of the plot corresponds to values of \bar{a}_4 and \bar{a}_5 forbidden by positivity conditions on the $\pi\pi$ scattering amplitudes. These bounds were obtained in Ref. [8], and slightly improved in Ref. [39]. Translated to \bar{a}_4 and \bar{a}_5 they read:

$$\bar{a}_5 + 2\bar{a}_4 \geq \frac{157}{40} \quad , \quad \bar{a}_4 \geq \frac{27}{20} . \quad (20)$$

Let us comment the most relevant features of the results of Figure 4:

- i/ No vector resonances are found for $\bar{a}_4 \lesssim 8$ and $\bar{a}_5 \lesssim 25$. This would exclude to a large extent Higgsless

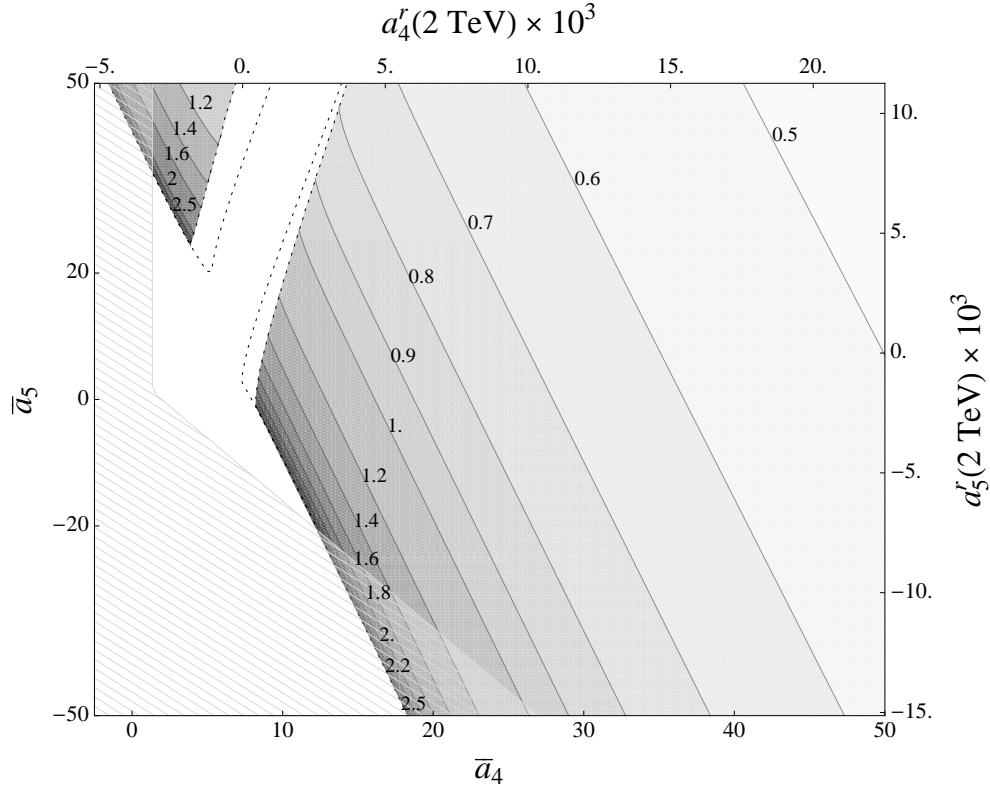


FIG. 4. Resonance masses as a function of the low-energy couplings \bar{a}_4 and \bar{a}_5 . The scales in terms of the renormalized couplings $a_4^r(\mu)$ and $a_5^r(\mu)$ at $\mu = 2$ TeV are also drawn. The shaded areas show where resonances defined by the conditions (7) and (19) with $\lambda = 1/3$ are found in the (\bar{a}_4, \bar{a}_5) -plane. The contour lines drawn correspond to pairs of (\bar{a}_4, \bar{a}_5) which yield the same resonance mass. The hatched region in the left and lower parts of the plot, given by Eq. (20), corresponds to values of \bar{a}_4 and \bar{a}_5 forbidden by positivity conditions on the $\pi\pi$ scattering amplitudes. The outermost dashed lines mark the boundary of the resonance region corresponding to $\lambda = 1/2$.

models with vector resonances which saturate the low-energy couplings to the expected natural order of magnitude ($\bar{a}_{4,5} \sim 1$).

- ii/ Masses above 1.8 TeV are confined to a thin slice in the lower-left and upper-left parts of the shaded regions and are mostly excluded by the positivity constraints. Conversely, light resonances ($\lesssim 0.8$ TeV) require values of either \bar{a}_4 or \bar{a}_5 larger than 20. The validity of the EChET Lagrangian for such large values of the LECs is nevertheless questionable and could indicate that additional degrees of freedom linked to the Goldstone boson dynamics are missing in the effective description.
- iii/ The dependence on the λ -cut is visible in the upper part ($\bar{a}_5 \gtrsim 0$) of the boundary of the allowed region for resonances, where the $\lambda = 1/2$ contour departs from the $\lambda = 1/3$ one, which defines the shaded region. Making the cut smaller would further constrain the region where resonances are found. We nevertheless think that the value $\lambda = 1/3$ is a realistic one, since it provides a reasonable suppression of S-waves and it is also found in the QCD case for the $\rho(770)$ resonance.
- iv/ For resonance masses $M_R \lesssim 0.8$ TeV, where either \bar{a}_4

or \bar{a}_5 are large, the formula:

$$M_R = v \left(\frac{192 \pi^2}{-11 + 10 \bar{a}_4 + 2 \bar{a}_5} \right)^{1/2}, \quad (21)$$

provides an approximation to the resonance masses in Figure 4 with an accuracy better than 10%. The formula (21) corresponds to the zero contours obtained by setting the loop functions $\bar{J}(x)$ in $A(t, s, u)$ to zero, and further neglecting the mass M .

- v/ A final consistency check for our method is provided by the Eq. (10) for the $I = 1$ P-wave phase-shift δ_1^1 . We evaluated the energy at which $\delta_1^1 = \pi/2$ for each value of the parameters \bar{a}_4, \bar{a}_5 in the shaded region of Figure 4 and we found that the result is basically the same we obtained from the condition in Eq. (7). Indeed, if we allow for at most a 10% deviation between both mass determinations, only the points in a tiny slice lying exactly on the boundary of the lower-half part of the big shaded region (in fact mostly excluded already by the positivity constraints) fail to pass the test. This result confirms that the S-wave background is indeed small, and therefore that the condition $\text{Re } z_0(M_R^2) \simeq 0$ is a

characteristic signature for vector resonances. As it was commented in relation with Figure 2, this result does not depend, essentially, on our knowledge of the $\delta_0^2(s)$ phase shift. It is enough that this is small with respect to the $\delta_1^1(s)$ phase shift at $E \simeq M_R$.

The LHC sensitivity to explore the values of the coefficients a_4 and a_5 has been investigated in Ref. [37]. The reported limits imply that in the combined region $\bar{a}_4 \lesssim 35$ and $-38 < \bar{a}_5 < 45$ no deviation from the SM prediction could be observed at the LHC. The prospects of measuring these parameters with improved accuracy in a high-luminosity e^+e^- collider operating at 1 TeV are slightly better [40]. On the other hand, the present bounds on new neutral vector resonances obtained recently [41] using ATLAS and CMS data, which exclude masses up to 1-2.3 TeV depending on their couplings and widths, could be used in combination with our results in Figure 4 to constrain the allowed regions of \bar{a}_4 and \bar{a}_5 which can accommodate a vector-saturated model.

A systematic study of resonance masses in the parametric space spanned by $a_4^r(\mu)$ and $a_5^r(\mu)$ using the Inverse Amplitude Method has also been performed [42, 43]. Their results, compared with our Figure 4, look rather different. From the pole of the Padé-improved P-wave they find for the vector resonance masses the result:

$$M_R = v \left(\frac{144 \pi^2}{3 \bar{a}_4 - 3 \bar{a}_5 + 1} \right)^{1/2}, \quad (22)$$

that can be compared with our Eq. (21), though the latter is only valid for large values of \bar{a}_4, \bar{a}_5 , i.e. for $M_R \gtrsim 0.8$ TeV. The slope of the lines of equal mass do not agree. Moreover, formula (22) forbids vector resonances in the region defined by $\bar{a}_5 > \bar{a}_4 + 1/3$, where their existence is consistent with our conditions. Also we note that the results of [42, 43] predict resonances in the region of $\bar{a}_{4,5} \sim 1$, that contradict our findings. A detailed comparative analysis between both methods in order to trace the origin of the discrepancies shall be carried out elsewhere.

V. CONCLUSION

Under the assumption that no light SM Higgs will be found at the LHC, we have investigated a method to identify vector resonances originated from a strong electroweak symmetry-breaking sector in the 1 TeV energy region. These resonances have become a possible alternative to the SM Higgs in preventing the seeming loss of perturbative partial-wave unitarity in the elastic scattering of the longitudinal components of W and Z gauge bosons. More important is that those resonances would provide a clear signal that a strong interacting dynamics is responsible for the spontaneous breaking of the electroweak symmetry.

We have focused, in particular, on the resonances that could contribute to the $W_L Z_L \rightarrow W_L Z_L$ scattering. This channel has the appropriate characteristics to implement our approach, that searches for vector resonances dominating the amplitude. Assuming resonance saturation of the LECs of the effective

chiral Lagrangian describing the interaction among Goldstone bosons, we could extract relevant information on the lightest vector resonances from the zeros of the elastic scattering amplitude. We first applied our method to the well known case of the $\rho(770)$ resonance and the $\mathcal{O}(p^4)$ chiral $\pi^- \pi^0 \rightarrow \pi^- \pi^0$ amplitude and considered the impact of introducing the next order in the chiral expansion.

Turning to the electroweak case we exploited the fact that, at leading order in the expansion provided by the equivalence theorem, the dynamics of the longitudinally polarized gauge boson scattering is described by the electroweak chiral Lagrangian (12), which is identical to the one that generates the $\rho(770)$ in elastic $\pi\pi$ scattering upon the obvious change of scale $F_\pi \rightarrow v$. Within this approach we have explored the parameter space of the two low-energy couplings \bar{a}_4 and \bar{a}_5 needed to describe the $W_L Z_L \rightarrow W_L Z_L$ scattering amplitude, in order to identify the region where a vector resonance can dominate the amplitude, and provide an estimate of its mass. The outcome has been shown in Figure 4 as a contour plot in the (\bar{a}_4, \bar{a}_5) -plane. Our main conclusion is that no vector resonances are found for $\bar{a}_4 \lesssim 8$ and $\bar{a}_5 \lesssim 25$, indicating that Higgsless models with vector resonances which saturate the low-energy couplings to the expected natural order of magnitude ($\bar{a}_{4,5} \sim 1$) would be excluded to a large extent. If we consider the neighborhood outside that natural order of magnitude, we see that the first resonances, appearing for $\bar{a}_4 \gtrsim 8$, have masses above 1 TeV. Lighter vector resonance masses appear for rather unnatural values of the parameters.

The improvement of our method by the inclusion of the $\mathcal{O}(p^6)$ contributions will entail a few technical difficulties, since it carries many new couplings (as it was seen in the QCD case in Section II) that make an analogous treatment to the one proposed here rather cumbersome. Nevertheless, if LHC confirms that there is no light Higgs, the study of the zeros of the gauge boson scattering amplitudes with the use of effective field theories driven by the spontaneous symmetry breaking pattern could provide a model-independent tool to explore the role of the resonances emerging from the new strong dynamics and shall therefore be pursued, for instance, through the search for higher spin states.

ACKNOWLEDGEMENTS

We wish to thank M.R. Pennington and A. Pich for comments and suggestions on the writing of this article, A. Pich for conversations on this topic and G. Ecker for his insight on the chiral $\mathcal{O}(p^6)$ LEC estimates. This project is partially supported by MEC (Spain) under grants FPA2007-60323 and FPA2011-23778, by the Spanish Consolider-Ingenio 2010 Programme CPAN (CSD2007-00042) and by Generalitat Valenciana under grant PROMETEO/2008/069.

Appendix A: Convergence of the partial-wave expansion in elastic $\pi\pi$ scattering

The partial-wave expansion of the elastic $\pi\pi$ scattering amplitude for a fixed s is defined in the real interval $z = [-1, 1]$, but it can be analytically continued to a larger region in the complex z -plane, according to a well-known theorem by K. Neumann (see *e.g.* Ref. [44]). The theorem states that the expansion of a function $f(z)$ in a series of Legendre polynomials is absolutely convergent in the interior of the largest ellipse with foci at $z = \pm 1$ in which $f(z)$ is analytic, and divergent in the exterior of the ellipse. In our case $f(z)$ is the $\mathcal{O}(p^4)$ chiral amplitude $A(t(s, z), s, u(s, z))$, Eq. (8), which for a fixed s has branch discontinuities at the t -channel and

u -channel thresholds, *i.e.* at $t = 4M^2$ and $u = 4M^2$. In the complex z -plane this translates to branch cuts extending from $z_+ = 1 + 8M^2/(s - 4M^2)$ to $+\infty$ and from $(-z_+)$ to $-\infty$. The region of convergence of the partial-wave expansion for $A(t(s, z), s, u(s, z))$ is thus an ellipse with foci at $z = \pm 1$ and semi-major axis z_+ . The semi-minor axis of the ellipse of convergence is equal to

$$z_- = \sqrt{z_+^2 - 1} = \frac{4M\sqrt{s}}{s - 4M^2}, \quad (\text{A.1})$$

and limits the size of the imaginary part of z for which the partial-wave series converges. Incidentally, for $M = 0$ the ellipses contracts to the interval $z = [-1, 1]$ and, hence, the partial-wave expansion is not convergent for $\text{Im } z \neq 0$.

-
- [1] M. Veltman, *Acta Phys. Polon.* **B8** (1977) 475.
 - [2] B. W. Lee, C. Quigg, and H. Thacker, *Phys. Rev. Lett.* **38** (1977) 883–885.
 - [3] H. G. Veltman and M. Veltman, *Acta Phys. Polon.* **B22** (1991) 669–696.
 - [4] S. Weinberg, *Physica* **A96** (1979) 327.
 - [5] J. Gasser and H. Leutwyler, *Annals Phys.* **158** (1984) 142.
 - [6] G. Ecker, J. Gasser, A. Pich, and E. de Rafael, *Nucl. Phys.* **B321** (1989) 311.
 - [7] M. Pennington, *AIP Conf. Proc.* **13** (1973) 89–116.
 - [8] M. Pennington and J. Portolés, *Phys. Lett.* **B344** (1995) 399–406.
 - [9] J. M. Cornwall, D. N. Levin, and G. Tiktopoulos, *Phys. Rev.* **D10** (1974) 1145.
 - [10] A. C. Longhitano, *Phys. Rev.* **D22** (1980) 1166.
 - [11] A. C. Longhitano, *Nucl. Phys.* **B188** (1981) 118.
 - [12] T. Appelquist and G.-H. Wu, *Phys. Rev.* **D48** (1993) 3235–3241.
 - [13] A. Martin and T. Spearman, *Elementary Particle Theory* (North-Holland Pub. Co., Amsterdam, 1970).
 - [14] B. Martin, D. Morgan, and G. Shaw, *Pion-Pion Interactions in Particle Physics* (Academic Press, London, 1976).
 - [15] A. Dobado, A. Gómez-Nicola, A. L. Maroto, and J. Peláez, *Effective lagrangians for the standard model* (Springer, Heidelberg, 1997).
 - [16] M. Pennington and P. Pond, *Nuovo Cim.* **A3** (1971) 548–560.
 - [17] M. Pennington and S. Protopopescu, *Phys. Rev.* **D7** (1973) 1429–1441.
 - [18] M. Pennington and C. Schmid, *Phys. Rev.* **D7** (1973) 2213–2219.
 - [19] R. Odorico, *Phys. Lett.* **B38** (1972) 411–414.
 - [20] E. Barrelet, *Nuovo Cim.* **A8** (1972) 331–371.
 - [21] M. Pennington and S. Protopopescu, *Phys. Lett.* **B40** (1972) 105–108.
 - [22] J. Gasser and H. Leutwyler, *Nucl. Phys.* **B250** (1985) 465.
 - [23] A. Pich, I. Rosell, and J. J. Sanz-Cillero, *JHEP* **1102** (2011) 109.
 - [24] D. Gómez Dumm, P. Roig, A. Pich, and J. Portolés, *Phys. Lett.* **B685** (2010) 158–164.
 - [25] S. Weinberg, *Phys. Rev. Lett.* **17** (1966) 616–621.
 - [26] J. Bijnens, G. Colangelo, G. Ecker, J. Gasser, and M. Sainio, *Nucl. Phys.* **B508** (1997) 263–310.
 - [27] J. Bijnens, G. Colangelo, and G. Ecker, *Annals Phys.* **280** (2000) 100–139.
 - [28] J. Gasser, C. Haefeli, M. A. Ivanov, and M. Schmid, *Phys. Lett.* **B675** (2009) 49–53.
 - [29] V. Cirigliano, G. Ecker, M. Eidemüller, R. Kaiser, A. Pich, and J. Portolés, *Nucl. Phys.* **B753** (2006) 139–177.
 - [30] S. Protopopescu, M. Alston-Garnjost, A. Barbaro-Galtieri, S. M. Flatte, J. Friedman, *et al.*, *Phys. Rev.* **D7** (1973) 1279.
 - [31] W. Ochs, *Thesis submitted to the University of Munich* (1973).
 - [32] P. Estabrooks and A. D. Martin, *Nucl. Phys.* **B79** (1974) 301.
 - [33] J. Gasser and U. G. Meissner, *Phys. Lett.* **B258** (1991) 219–224.
 - [34] A. Schenk, *Nucl. Phys.* **B363** (1991) 97–116.
 - [35] A. Arneodo, F. Guerin, and J. Donohue, *Nuovo Cim.* **A17** (1973) 329–342.
 - [36] A. Dobado and J. Peláez, *Nucl. Phys.* **B425** (1994) 110–136.
 - [37] O. Éboli, M. González-García, and J. Mizukoshi, *Phys. Rev.* **D74** (2006) 073005.
 - [38] M. Fabbrichesi and L. Vecchi, *Phys. Rev.* **D76** (2007) 056002.
 - [39] A. V. Manohar and V. Mateu, *Phys. Rev.* **D77** (2008) 094019.
 - [40] E. Boos, H. He, W. Kilian, A. Pukhov, C. Yuan, *et al.*, *Phys. Rev.* **D61** (2000) 077901.
 - [41] O. Éboli, J. González-Fraile, and M. González-García, *Phys. Rev.* **D85** (2012) 055019. 10 pages, 6 figures.
 - [42] A. Dobado, M. Herrero, J. Peláez, and E. Ruiz Morales, *Phys. Rev.* **D62** (2000) 055011.
 - [43] J. Peláez, *Phys. Rev.* **D55** (1997) 4193–4202.
 - [44] P. J. Davis, *Interpolation and Approximation*. Dover Publications, New York, first ed., 1975.